Preprints of the 21st IFAC World Congress (Virtual)
Berlin, Germany, July 12-17, 2020

Hybrid Cybernetic Modeling of Polyhydroxyalkanoate Production in *Cupriavidus necator* using Fructose and Acetate as Substrates

Stefanie Duvigneau * **Robert Dürr** ** **Lisa Carius** *
Achim Kienle *,**

* *Institute for Automation Engineering, Otto von Guericke University Magdeburg*
** *Process Synthesis and Process Dynamics, Max Planck Institute for Dynamics of Complex Technical Systems, Magdeburg*

Abstract: Due to their advantageous properties, polyhydroxyalkanoates are a promising alternative to conventional petroleum-based plastics. Currently, high production costs in upstream and downstream have to be reduced to make the plastic material competitive. As most of the PHA producing organisms metabolize a wide range of substrates upstream cost can be reduced using carbon rich waste material. For large scale application sophisticated control approaches based on mathematical models can help to further increase the productivity. In the present work, a hybrid cybernetic model approach is presented, which is adapted to experiments with fructose and acetate feeding, respectively. Furthermore, the validated model was used to qualitatively predict the effect of co-substrate feeding.

Keywords: Polyhydroxyalkanoates, Hybrid cybernetic modeling, Metabolic yield analysis, *Cupriavidus necator*, Fructose, Acetate

1. INTRODUCTION

Besides petroleum-based polymers, the group of polyhydroxyalkanoates (PHAs) represents promising raw material for production of plastics. PHA-based materials are biodegradable, non-toxic and bio-based, since these polymers can be accumulated by a broad range of microorganisms caused by limitation of, e.g., nitrogen, phosphorus or oxygen (Raza et al., 2018). Probably the best studied representative from the class of PHAs is polyhydroxybutyrate (PHB). PHB is a homopolymer of the short-chain fatty acid (scl fatty acid) hydroxybutyrate (HB) which is produced by a variety of microorganisms from organic material. The most prominent producer is the bacterium *Cupriavidus necator* (*C. necator*), which was also used in this work.

One major goal to make PHA-based plastics economically competitive, is to reduce the costs of the fermentation process by inexpensive substrates (Koller et al., 2010). Furthermore, through smart process control and the combination of different substrates, productivity of the bioprocess can be improved (Carius et al., 2018; Morabito et al., 2019; Lopar et al., 2013; Špoljarić et al., 2013). These approaches require sophisticated mathematical process descriptions. Hybrid cybernetic models (HCMs) combine stoichiometric information of metabolic networks with temporal dynamics and are therefore promising candidates (Ramkrishna and Song, 2018). Thus, more a priori knowledge is used in HCMs in comparison to simple kinetic models. Furthermore, cellular regulatory mechanisms are considered without modeling them in detail. For that purpose cybernetic variables are introduced to regulate enzyme activity and synthesis.

In the present work, we develop an HCM considering fructose and acetate, two common substrates for the PHB production by combining two metabolic models of *C. necator* from literature (Franz et al., 2011; Yu and Si, 2004). Previous work for other microorganisms has already shown that HCMs are suitable for studying co-substrates (Song et al., 2009a). This is the first time, where the HCM approach with co-substrate feeding is applied to the field of biopolymer production in *C. necator*.

First, an adaption of the HCM rate constants $\mathbf{k_r}$ to two different data sets is performed by using the data obtained after feeding with single carbon sources fructose and acetate, respectively. An analysis of the theoretically possible yield space and experimental yields with respect to total biomass and HB is provided. Furthermore, the time evolutions for single carbon substrate feedings are shown. Finally, simulations w.r.t. the maximum HB concentration for the co-feeding are performed. Different ratios of fructose and acetate are assumed in the *in silico* study.

2. EXPERIMENTAL METHODS

2.1 Mircoorganism and cultivation conditions

The experiments were performed with *C. necator* (H16, DSM 428) obtained from DSMZ GmbH Braunschweig. For the experiment with acetate as a single carbon substrate, a 1 L shake flask was filled with 200 mL of culture. M81 me-

dia [1] were supplemented with 10 g/L sodium acetate and 1.5 g/L ammonium chloride (both: Carl Roth, Karlsruhe) and inoculated with *C. necator* H16, precultured in LB media. The initial optical density of the culture was set to 0.4. The culture was incubated at 30 °C and 150 rpm for 120 hours (h). Samples were taken every 8 h and analysed as described below. In contrast, for fructose as a single carbon substrate, no new experiments were performed but the data of Franz et al. (2011) obtained with the same strain were used.

2.2 Enzyme Assay

The ammonium and fructose concentrations were determined from supernatant of the samples using an enzymatic test kits (Kit No. 5390 and No. 10139106035, R-Biopharm AG, Darmstadt, Germany) and following the manufactures instructions.

2.3 High pressure liquid chromatography

Acetate and HB concentrations were determined with an Agilent 1100 high performance liquid chromatography (HPLC). For acetate 10 μL of the filtered supernatants were loaded on reversed phase column (Inertsil 100A ODS-3, 5μm pore size, 250x4.6mm, MZ-Analysentechnik GmbH, Mainz, Germany) and eluted isocratically with 1mL·min^{-1} and 0.1M $NH_4H_2PO_4$ at pH 2.6 and 40 °C.
For the determination of the HB concentration 1 mL culture broth was alkaline digested and prepared as reported in (Satoh et al., 2016). 10μL of the digested and filtered samples were loaded on the reverese phase column (see above) and eluted isocratically with 1mL·min^{-1} at 60 °C. The eluent consists of 92% low concentrated H_2SO_4 (0.025% solution, Carl Roth, Karlsruhe) and 8% acetonitrile (Carl Roth, Karlsruhe). The HB concentration of the samples was determined by crotonic acid standards (Carl Roth, Karlsruhe). Since the alkaline digestion is not a perfect conversion from HB to crotonic acid, a PHB sample (Sigma Aldrich, St. Louis) with known concentration must additionally be processed to calculate a conversion yield Y_{HB} (Satoh et al., 2016):

$$Y_{HB} = \frac{c_{CA}}{c_{HB}} \cdot D \tag{1}$$

Here, the dilution ratio is $D = 2$ (1:2 v/v) and c_{HB} is the known HB concentration of the test sample. The concentration of crotonic acid c_{CA} is determined by the processed crotonic acid standard.
For both procedures peaks were detected with a photodiode-array detector (G7115A, Agilent, Waldbronn, Germany).

2.4 Determination of Cell Dry Weight

For the determination of total cell dry weight, 1 ml culture broth was centrifuged in pre-weighed plastic tubes for 10 minutes at 13000 x g and 4 °C. Subsequently, the cell pellet was dried for 1 h at 99 °C and weighed.

3. MATHEMATICAL MODEL

3.1 Metabolic model

The present metabolic model (Appendix B) is based on models of Franz and co-authors (Franz et al., 2011) as well as Yu and Si (2004). By combining both, the resulting model was expanded to the two substrate inputs fructose and acetate. Furthermore, the reversibility of reaction equations was checked and adjusted using the KEGG database.

3.2 Metabolic yield analysis

Metabolic yield analysis was performed as described by Song and Ramkrishna (2009). First, the elementary modes of the network have to be calculated. In the present work, 4857 elementary modes were calculated using *Metatool*. As suggested by Song and co-authors (Song et al., 2009a), the elementary modes of the metabolic model were classified into different sub-models according to the input substrates in order to preserve functionality of the overall model. Subsequently, the elementary modes for each sub-model were reduced to a set of GMs by designing the convex hull of the elementary modes in the yieldspace of HB and biomass via the *MATLAB* command *convhulln*. For further information regarding the analysis in yield space we refer to the publication of Song and Ramkrishna (2009). For the presented model, 38 relevant GMs were selected to describe the process dynamics.
GMs were further reduced by selecting active modes relevant to experimental data. In the present work, selection was done during the parameter estimation. The set of GMs with the lowest normalized error square sum (ESS, (2)) was selected as AM set (N=15) shown in Table 1. The AMs reflect all possible metabolic states during HB synthesis in *C. necator*. In addition to the AMs that produce biomass, HB or acetate, there are three other modes accounting for cellular maintenance (AM 2, 11 and 14). Here, HB is metabolized to residual biomass and energy. This process produces CO_2 (not shown in Table 1). Maintenance can be considered in the absence of all external carbon sources (AM 14) or if the uptake of the substrate is reduced (AM 2 and AM 11).

$$ESS = \sum_{i=1}^{n} \left(\frac{\mathbf{x_{exp}}(t_i) - \mathbf{x_{sim}}(\mathbf{t_i})}{max(\mathbf{x_{exp}})} \right)^2 \tag{2}$$

To calculate the ESS, the difference between n simulated and experimental data points (x_{sim} and x_{exp}) at time t_i was calculated, weighted with the maximum experimental value and summed up. The variable $\mathbf{x}$ is defined as $\mathbf{x} = [x_{fru},\ x_{ace},\ x_N,\ x_{HB},\ x_c]$.

3.3 State equation

State equations for the given input substrates fructose (x_{fru}), acetate (x_{ace}) and ammonium (x_N) are defined as follows:

$$\frac{d}{dt} \begin{bmatrix} x_{fru} \\ x_{ace} \\ x_N \end{bmatrix} = \mathbf{S_s Z r_M c} \tag{3}$$

The stoichiometric information and selected AMs of the metabolic network are included by the AM matrix in yield space $\mathbf{S_s Z}$. Furthermore, the influence of various substrate concentrations for each AM is modeled with Monod-type kinetic in $r_{M,i}$ (9).
In addition to the equations for the substrates, differential equations for internal metabolites with slow dynamics compared to the remaining internal metabolites can also be described (Franz et al., 2011). This assumption holds

[1] Recipes for the Medium 81 can be found in Franz et al. (2011) or on the web page of the DSMZ.

e.g. for cellular storage materials such as PHB. The dynamics of the HB content m_{HB} can be described as

$$\frac{dm_{HB}}{dt} = \mathbf{S_{HB}Z r_M} - \mu \mathbf{m_{HB}}, \tag{4}$$

where $\mathbf{S_{HB}Z}$ describes the AM matrix with respect to HB in yield space and μ the cellular growth rate.

A special feature of the hybrid cybernetic approach is the use of enzymes for each theoretical AM:

$$\frac{d\mathbf{e}}{dt} = \alpha + \mathbf{r_{EM}}b - \beta\mathbf{e} - \mu\mathbf{e}, \tag{5}$$

where

$$e_i^{\text{rel}} = \frac{e_i}{e_i^{\max}} \text{ with } e_i^{\max} = \frac{\alpha_i + k_{e,i}}{\beta_i + k_{r,i}(\mathbf{S_cZ})_\mathbf{i}}. \tag{6}$$

The increase of the enzyme level occurs via the constitutive enzyme synthesis rate α and the catalytically active part of the total biomass b. The catalytically active biomass fraction is controlled by Monod-type kinetics (10). Enzymes are degraded by the rate β and diluted due to cell growth (μ). The state equation for the total biomass concentration c can be described as follows:

$$\frac{dc}{dt} = \mu c. \tag{7}$$

The growth rate μ is defined by the rate vector $\mathbf{r_M}$ and the AM matrix for the biomass in yield space $\mathbf{S_cZ}$:

$$\mu = \mathbf{S_cZ r_M}. \tag{8}$$

In general, the rates r_M and r_{EM} for the ith AM are defined as:

$$r_{M,i} = v_i k_{r,i} e_i^{\text{rel}} r_{\text{core,i}}, \tag{9}$$

$$r_{EM,i} = u_i k_{e,i} r_{\text{core,i}}. \tag{10}$$

The rate r_{core} of the ith AM is a multiplied Monod-type kinetic:

$$r_{\text{core,i}} = \frac{X_1}{K_{X_1} + X_1} \cdot \ldots \cdot \frac{X_n}{K_{X_n} + X_n}. \tag{11}$$

The substrate index n (fructose, acetate, ammonium) depend on the number of negative yield coefficients for each AM given in Table 1. Besides the Monod-type kinetic, cybernetic control variables u and v which regulate enzyme synthesis and enzyme activity, respectively, are calculated by cybernetic control laws (Young and Ramkrishna, 2007):

$$\mathbf{u} = \frac{\mathbf{p}}{\|\mathbf{p}\|_\mathbf{1}} \qquad \mathbf{v} = \frac{\mathbf{p}}{\|\mathbf{p}\|_\infty}. \tag{12}$$

Here, $\mathbf{p}$ is the return on investment which can be calculated as follows:

$$\mathbf{p} = \text{diag}(\mathbf{f_c})\text{diag}(\mathbf{e}^{\text{rel}})\text{diag}(\mathbf{k_r})\mathbf{r}_{\text{core}} \tag{13}$$

The vector of uptaken carbon units $\mathbf{f_c}$ is normalized with respect to the highest carbon uptake. The vector is shown in Table 1.

3.4 Parameters

Since the system was extended by enzyme equations for the AMs and an adapted Monod kinetic for each mode on the basis of our previous work (Franz et al., 2011), only the constants $k_{r,i}$ in the definition of the rate $r_{M,i}$ are free model parameters to be estimated from experimental data. All other parameters of the model were kept as given in Franz et al. (2011). The uptake of the carbon source acetate is known to accelerate metabolism (Garcia-Gonzalez and De Wever, 2018). Therefore, the saturation constant K_{ACE} is assumed as $K_{\text{FRU}}/2$. All parameter values are given in Table 2.

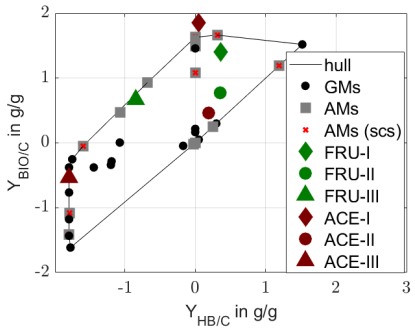

Fig. 1. **Yield space of carbon-normalized HB and total biomass.** Experimental yields are divided into different phases (see text) for the carbon sources fructose (FRU) and acetate (ACE). The grey squares are the selected active modes (AMs) and the red crosses are those AMs, that are used to adapt on experiments with single carbon source (scs).

3.5 Numerical solution and parameter estimation

The model was implemented and solved numerically in *MATLAB2016b*. Parameter adjustment of rates k_r were performed using the *MATLAB* routine *fmincon* with a lower bound of zero on all model parameters. Furthermore, as the optimization problem is highly nonlinear, a multi-start optimization approach with $n = 100$ random initial parameter estimates was implemented to reduce the risk of ending up in a local extremum when minimizing the cost function described in Equation (2).

4. RESULTS

In the present work an HCM was developed, which can describe the growth and the HB accumulation with either fructose or acetate as carbon source. Figure 1 shows the yield space for carbon-normalized HB and total biomass as well as the experimental yields. Two data sets were used to adjust the parameters of the model: one data set with fructose as carbon source from literature (Franz et al., 2011) and another with acetate as carbon source from our own shake flask experiment. Both data sets have been divided into different phases for the calculation of yields:

- Phase I: exponential growth
- Phase II: HB accumulation
- Phase III: HB consumption

The position of experimental yields in Figure 1 gives an indication about the model fit to describe the data. Yields for data sets with fructose as carbon source are inside or on the theoretical hull spanned by metabolic model. Due to the high uncertainty in the measurement of small dry biomass and the broad sampling time interval for the data set with acetate as the carbon source, the yields for phase I and III are on the edge or slightly outside the hull.

In the following, a parameter estimation was performed for the constants $k_{r,i}$, whose Monod-type kinetics in $r_{M,i}$ can describe the growth on single carbon substrates. All remaining constants $k_{r,i}$ have been set to zero, as the co-substrate feeding was not investigated experimentally. The AMs that were included in the adjustment are marked in the yield space (Figure 1, crosses in gray squares) and in Table 1 (FRU, ACE).

Table 1. **Values for the yields in g/gC of the active mode matrix subdivided into different subsections:** substrates $S_S Z$ (1, upper white entries), HB $S_{HB} Z$ (2, light grey entries) and total biomass $S_c Z$ (3, grey entries). Furthermore the normalized vector of uptaken carbon units $\mathbf{f_c}$ and division of AMs for the submodels fructose (FRU) and acetate (ACE) are shown.

AM		1	2	3	4	5	6	7	8	9	10	11	12	13	14	15
Y_{fru}		-2.50	-0.28	-2.50	-2.44	-1.00	-1.29	-2.50	-1.56	-2.50	0.00	0.00	0.00	0.00	0.00	-2.50
Y_{ace}	(1)	0.00	0.00	0.00	-0.06	-0.01	-1.19	0.30	0.01	0.06	0.43	-0.01	-2.46	-2.46	0.00	0.00
Y_N		-0.64	-0.73	0.00	-0.75	-0.72	0.00	-0.70	-0.76	0.00	-0.18	-0.33	-0.51	0.00	-0.001	-0.77
Y_{HB}	(2)	0.31	-1.59	1.19	0.00	-1.07	0.25	0.00	-0.68	0.00	-1.79	-1.78	0.00	1.19	-0.021	0.00
Y_c	(3)	1.66	-0.05	1.19	1.58	0.47	0.25	1.49	0.93	0.00	-1.42	-1.08	1.08	1.19	-0.018	1.63
$\mathbf{f_c}$		1.00	0.75	1.00	1.00	0.83	0.99	1	0.89	1.00	0.72	0.72	0.98	0.98	0.01	1.00
Submodel		FRU	FRU	FRU							ACE	ACE	ACE	ACE	FRU	FRU

Table 2. Parameters of the HCM

Constant	Value
$\mathbf{k_r}$ [1/h] [1]	[0.26 3.71 0.07 $\mathbf{0}^{1x6}$ 3.44 1.51 0.44 0.44 0.44 0.25]^T
$\mathbf{k_e}$ [1/h]	$\mathbf{0.1}^{15x1}$
$\boldsymbol{\alpha}$ [1/h]	$0.01\mathbf{k_e}$
$\boldsymbol{\beta}$ [1/h]	$\mathbf{5}^{15x1}$
K_N [g/L]	0.01
K_{FRU} [g/L]	0.06
K_{ACE} [g/L]	0.03
K_{HB} [g/L]	0.05

[1] estimated values, arranged according to Table 1

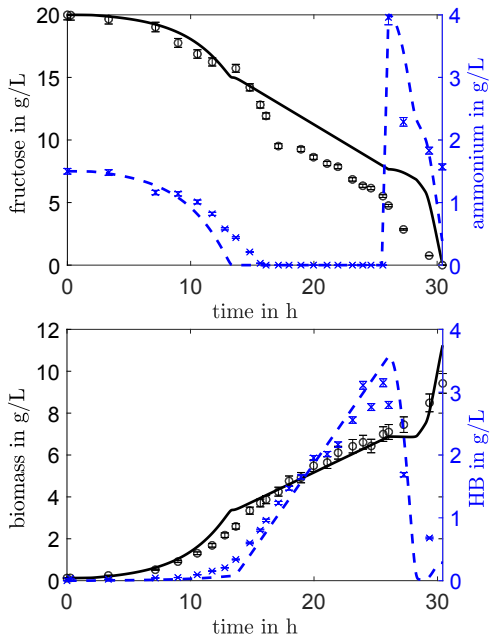

Fig. 2. **Dynamic behaviour using 20 g/L fructose as carbon source.** Experimental (circles and crosses) and model kinetics (solid and dashed lines) of fructose (upper black line and circles), ammonium (upper dashed blue line and crosses), total biomass (bottom black line and circles) and hydroxybutyrate (HB, bottom dashed blue line and crosses) concentrations are shown.

Figure 2 and 3 show the simulated dynamics after parameter adjustment for both data sets. In the case of fructose as single carbon substrate (Figure 2), the model can reproduce the data very well. An exception is the fructose concentration, which decreases exponentially up to approximately 18 h, but in the simulation only up to

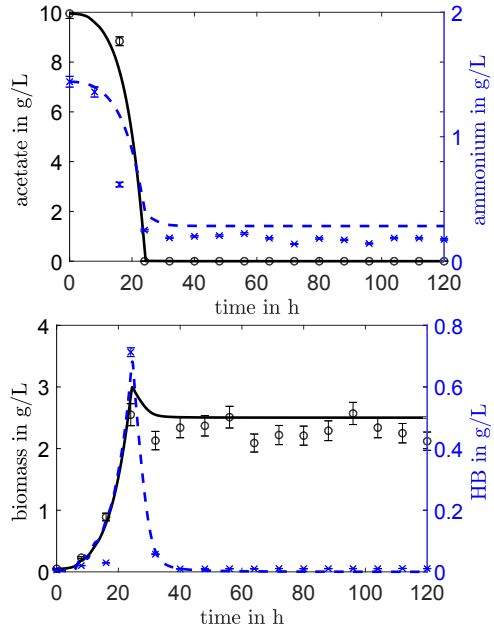

Fig. 3. **Dynamic behaviour using 10 g/L acetate as carbon source.** Experimental (circles and crosses) and model kinetics (solid and dashed lines) of acetate (upper black line and circles), ammonium (upper dashed blue line and crosses), total biomass (bottom black line and circles) and hydroxybutyrate (HB, bottom dashed blue line and crosses) concentrations are shown.

approximately 15 h. The linear phase in the model starts earlier, as the exponential decay of the substrate in the kinetics is coupled to ammonium, that is consumed after 15 h. The delayed start of linear substrate uptake in the experiment indicates that other metabolites such as organic acids are also generated at the beginning of the PHB production phase. In the future, additional measurements of the latter should be taken into account and included in an extended model formulation.

In case of acetate as a carbon source, the dynamics can be reproduced very well (Figure 3). Solely, the simulated residual ammonium concentration gives evidence that the linear relationship between biomass growth and ammonium consumption should be adjusted in later model variants by adjusting the stoichiometry in the biomass equation.

Finally, the adapted HCM was used to analyze the effect of fructose and acetate as co-substrates (Figure 4). Therefor, different carbon ratios of acetate/fructose are simulated

and compared regarding their maximum amount of HB. Our model predicts an benefical effect of co-feeding that is increased with an evaluated acetate concentration in the substrate mixture. A ratio of 1/10 acetate/fructose in the initial concentration predicts an improvement of 6% compared to the summed HB concentration for feeding with only one carbon source ($\max(\mathrm{HB})_{\mathrm{FRU}}+\max(\mathrm{HB})_{\mathrm{ACE}}$). With an 1/1 acetate/fructose ratio, the increase is already 45%. This effect is a valuable information for the combination of waste materials as carbon sources with respect to a cheap and productive process.

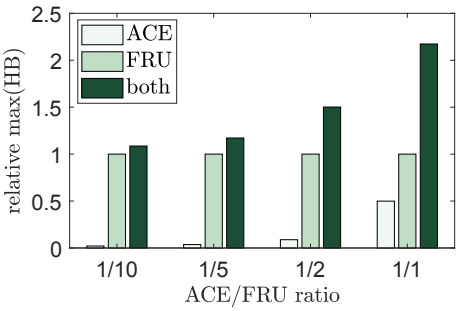

Fig. 4. **Relative maximum concentration of HB with different acetate/fructose (ACE/FRU) ratios.** The HB concentrations are normalized w.r.t. the maximum HB concentration in the simulation with fructose as the single carbon substrate.

5. CONCLUSION

In the present work, a HCM was developed and adapted to experimental data with fructose and acetate as a single carbon source. For this purpose, a metabolic yield analysis was performed in which the relevant AMs were determined (Song and Ramkrishna, 2009). This set of AMs is used to describe the rates of all state variables. Thus, the model has the advantage of being able to use the a priori information from the metabolic network for the simulation of the dynamics. In addition to the use of metabolic information, the HCM approach uses cybernetic variables. These cybernetic variables make it possible to describe the growth on several substrates in a proper way (Song et al., 2009a). Due to the lack of a suitable experimental data set for co-feeding, the HCM adapted on data with single feeding strategies was used for an *in silico* study with different acetate/fructose ratios. Therein, a positive effect on the HB yield at a given co-substrate feeding with fructose and acetate is predicted. This effect is already well-known for different experimental setups and organisms (Garcia-Gonzalez and De Wever, 2018; Karmann et al., 2019). In contrast to our predictions, Garcia-Gonzalez and De Wever (2018) also observed an inhibitory effect on biomass production when feeding 4 g/l or even higher concentrations of a feed containing only acetate. Future work will focus on experimental investigations and corresponding extension of our HCM to take such inhibitory effects into account.

Furthermore, the simulation results should be experimentally validated under controlled conditions. With such a validation experiment the remaining AMs considering the uptake of both, fructose and acetate, could be included in the HCM, as an expansion of the model. In addition, a sophisticated analysis of parametric inference, e.g. using parametric bootstraps or profile likelihoods (Raue et al., 2009), is planned.

After successful experimental validation, acetate can also be used in combination with low cost substrates (for example, regional waste products) to maximize PHA production and make the bio-based, biodegradable plastic material economically competitive to conventional plastic material. In addition, the hybrid model approach can be integrated into model-based control approaches to better control continuous bioprocesses for PHA production (Morabito et al., 2019).

ACKNOWLEDGEMENTS

We would like to acknowledge the EU-programme ERDF (European Regional Development Fund) for the funding of Stefanie Duvigneau as part of the project DIGIPOL. Furthermore we would like to thank Anja Julius for the support in laboratory.

Appendix A. METABOLITE ABBREVIATIONS

3PG	3-phosphoglycerate
αKG	alpha-ketoglutarate
ACE	acetate
AcACE	acetoacetate
AcAcCoA	acetoacetyl CoA
AcCoA	acetyl CoA
ADP	adenosine diphosphate
ATP	adenosine triphosphate
AMP	adenosine monophosphate
AMC	ammonium chloride
BIO	residual biomass
CO_2	carbon dioxide
E4P	erythrose-4-phosphate
F16P	fructose-1,6-bisphosphate
F6P	fructose-6-phosphate
FAD	flavin adenin dinucleotide, oxidized
FADH	flavin adenin dinucleotide, reduced
FRU	fructose
G3P	glyceraldehyde-3-phosphate
G6P	glucose-6-phosphate
GLN	glutamine
GLU	glutamate
GOX	glyoxylate
HB	hydroxybutyrate
ISC	isocitrate
MAL	malate
NAD	nicotinamide adenine dinucleotide (ox.)
NADH	nicotinamide adenine dinucleotide (red.)
NADP	nicotinamide adenine dinucleotide phosphate (ox.)
NADPH	nicotinamide adenine dinucleotide phosphate (red.)
NH_3	ammonia
O_2	oxygen
OXA	oxaloacetate
PEP	phosphoenol pyruvate
PYR	pyruvate
R5P	ribose-5-phosphate
Rl5P	ribulose-5-phosphate
S7P	sedoheptulose-7-phosphate
SUC	succinate
SucCoA	succinyl-CoA
SUCx	succinate, external
X5P	xylulose-5-phosphate

Appendix B. METABOLIC REACTIONS

No.	Reaction
1	FRU + PEP + ATP $\longrightarrow$ F16P + PYR + ADP
2	F16P $\longrightarrow$ F6P
3	F16P $\longleftrightarrow$ 2 G3P
4	AMC $\longrightarrow$ NH_3
5	G6P + 2 NADP $\longrightarrow$ Rl5P + CO_2 + 2 NADPH
6	Rl5P $\longleftrightarrow$ R5P
7	Rl5P $\longleftrightarrow$ X5P
8	X5P + R5P $\longleftrightarrow$ S7P + G3P
9	S7P + G3P $\longleftrightarrow$ E4P + F6P
10	X5P + E4P $\longleftrightarrow$ G3P + F6P
11	F6P $\longleftrightarrow$ G6P
12	G3P + NAD + ADP $\longleftrightarrow$ 3PG + NADH + ATP
13	3PG $\longleftrightarrow$ PEP
14	PEP + ADP $\longleftrightarrow$ PYR + ATP
15	OXA + ATP $\longleftrightarrow$ PEP + ADP + CO_2
16	PYR + NAD $\longleftrightarrow$ AcCoA + NADH + CO_2
17	AcCoA + OXA $\longleftrightarrow$ ISC
18	ISC + NADP $\longleftrightarrow$ αKG + NADPH + CO_2
19	αKG + NAD $\longrightarrow$ SucCoA + NADH + CO_2
20	SucCoA + ADP $\longleftrightarrow$ SUC + ATP
21	SUC $\longrightarrow$ SUCx
22	SUC + FAD $\longleftrightarrow$ MAL + FADH
23	MAL + NAD $\longleftrightarrow$ OXA + NADH
24	MAL + NADP $\longleftrightarrow$ PYR + CO2 + NADPH
25	PYR + ATP $\longrightarrow$ OXA + ADP
26	ISC $\longrightarrow$ SUC + GOX
27	AcCoA + GOX $\longrightarrow$ MAL
28	NH_3 + αKG + NADPH $\longleftrightarrow$ GLU + NADP
29	GLU + NH_3 + ATP $\longleftrightarrow$ GLN + ADP
30	2 AcCoA $\longleftrightarrow$ AcAcCoA
31	AcAcCoA + NADPH $\longrightarrow$ HB + NADP
32	ACE + ATP $\longleftrightarrow$ AcCoA + AMP
33	HB + NAD $\longleftrightarrow$ AcACE + NADH
34	ACE + SucCoA $\longleftrightarrow$ AcAcCoA + SUC
35	AcACE + ATP $\longrightarrow$ AcCoA + AMP
36	2 NADH + O_2 + 4 ADP $\longrightarrow$ 2 NAD + 4 ATP
37	ATP + AMP $\longleftrightarrow$ 2 ADP
38	2 FADH + O_2 + 2 ADP $\longrightarrow$ 2 FAD + 2 ATP
39	0.21 G6P + 0.07 F6P + 0.9 R5P + 0.36 E4P + 0.13 G3P + 1.5 3PG + 0.52 PEP + 2.83 PYR + 3.74 AcCoA + 1.79 OXA + 8.32 GLUT + 0.25 GLUM + 41.1 ATP + 8.26 NADPH + 3.12 NAD $\longrightarrow$ BIO + 7.51 αKG + 2.61 CO2 + 41.1 ADP + 8.26 NADP + 3.12 NADH (Katoh et al., 1999)

All stoichiometric coefficients are given in mmol, except BIO is given in g.

REFERENCES

Carius, L., Pohlodek, J., Morabito, B., Franz, A., Mangold, M., Findeisen, R., and Kienle, A. (2018). Model-based State Estimation Based on Hybrid Cybernetic Models. *IFAC-PapersOnLine*, 51(18), 197–202.

Franz, A., Song, H.S., Ramkrishna, D., and Kienle, A. (2011). Experimental and theoretical analysis of poly(β-hydroxybutyrate) formation and consumption in Ralstonia eutropha. *Biochemical Engineering Journal*, 55(1), 49–58.

Garcia-Gonzalez, L. and De Wever, H. (2018). Acetic acid as an indirect sink of CO2 for the synthesis of polyhydroxyalkanoates (PHA): Comparison with PHA production processes directly using CO2 as feedstock. *Applied Sciences (Switzerland)*, 8(9). doi:10.3390/app8091416.

Karmann, S., Panke, S., and Zinn, M. (2019). Fed-batch cultivations of rhodospirillum rubrum under multiple nutrient-limited growth conditions on syngas as a novel option to produce poly(3-hydroxybutyrate) (PHB). *Frontiers in Bioengineering and Biotechnology*, 7(59), 1–11.

Katoh, T., Yuguchi, D., Yoshii, H., Shi, H.D., and Shimizu, K. (1999). Dynamics and modeling on fermentative production of poly(β-hydroxybutyric acid) from sugars via lactate by a mixed culture of Lactobacillus delbrueckii and Acaligenes eutrophus. *Journal of Biotechnology*, 67(2-3), 113–134.

Koller, M., Atli, A., Dias, M., Reiterer, A., and Braunegg, G. (2010). *Microbial PHA Production from Waste Raw Materials*, volume 14. Springer-Verlag Berlin Heidelberg.

Lopar, M., Vrana Špoljarić, I., Atlić, A., Koller, M., Braunegg, G., and Horvat, P. (2013). Five-step continuous production of PHB analyzed by elementary flux, modes, yield space analysis and high structured metabolic model. *Biochemical Engineering Journal*, 79, 57–70.

Morabito, B., Kienle, A., Findeisen, R., and Carius, L. (2019). Multi-mode Model Predictive Control and Estimation for Uncertain Biotechnological Processes. *IFAC-PapersOnLine*, 52(1), 709–714.

Ramkrishna, D. and Song, H.S. (2018). *Cybernetic Modeling for Bioreaction Engineering*. Cambridge University Press.

Raue, A., Kreutz, C., Maiwald, T., Bachmann, J., Schilling, M., Klingmüller, U., and Timmer, J. (2009). Structural and practical identifiability analysis of partially observed dynamical models by exploiting the profile likelihood. *Bioinformatics*, 25(15), 1923–1929.

Raza, Z.A., Abid, S., and Banat, I.M. (2018). Polyhydroxyalkanoates: Characteristics, production, recent developments and applications. *International Biodeterioration and Biodegradation*, 126, 45–56.

Satoh, H., Sakamoto, T., Kuroki, Y., Kudo, Y., and Mino, T. (2016). Application of the Alkaline-Digestion-HPLC Method to the Rapid Determination of Polyhydroxyalkanoate in Activated Sludge. *Journal of Water and Environment Technology*, 14(5), 411–421.

Song, H.S., Morgan, J.A., and Ramkrishna, D. (2009a). Systematic development of hybrid cybernetic models: application to recombinant yeast co-consuming glucose and xylose. *Biotechnology and Bioengineering*, 103(5), 984–1002.

Song, H.S. and Ramkrishna, D. (2009). Reduction of a set of elementary modes using yield analysis. *Biotechnology and Bioengineering*, 102(2), 554–568.

Špoljarić, Ivna, V., Lopar, M., Koller, M., Muhr, A., Salerno, A., Reiterer, A., Malli, K., Angerer, H., Strohmeier, K., Schober, S., Mittelbach, M., and Horvat, P. (2013). Mathematical modeling of poly[(R)-3-hydroxyalkanoate] synthesis by Cupriavidus necator DSM 545 on substrates stemming from biodiesel production. *Bioresource Technology*, 133, 482–494.

Young, J.D. and Ramkrishna, D. (2007). On the Matching and Proportional Laws of Cybernetic Models. *Biotechnology Progress*, 23(1), 83–99.

Yu, J. and Si, Y.T. (2004). Metabolic carbon fluxes and biosynthesis of polyhydroxyalkanoates in Ralstonia eutropha on short chain fatty acids. *Biotechnology Progress*, 20(4), 1015–1024.